DOI 10.5012/bkcs.2010.31.11.3077

Articles

Anodic Stripping Voltammetric Detection of Arsenic(III) at Platinum-Iron(III) Nanoparticle Modified Carbon Nanotube on Glassy Carbon Electrode†

Seung-Hyun Shin and Hun-Gi Hong*

*Department of Chemistry Education , Seoul National University, Seoul 151-748, Korea. *E-mail: hghong@snu.ac.kr*
Received June 4, 2010, Accepted August 2, 2010

The electrochemical detection of As(III) was investigated on a platinum-iron(III) nanoparticles modified multiwalled carbon nanotube on glassy carbon electrode(nanoPt-Fe(III)/MWCNT/GCE) in 0.1 M H_2SO_4. The nanoPt-Fe(III)/MWCNT/GCE was prepared *via* continuous potential cycling in the range from −0.8 to 0.7 V (*vs*. Ag/AgCl), in 0.1 M KCl solution containing 0.9 mM K_2PtCl_6 and 0.6 mM $FeCl_3$. The Pt nanoparticles and iron oxide were co-electrodeposited into the MWCNT-Nafion composite film on GCE. The resulting electrode was examined by cyclic voltammetry (CV), scanning electron microscopy (SEM), and anodic stripping voltammetry (ASV). For the detection of As(III), the nanoPt-Fe(III)/MWCNT/GCE showed low detection limit of 10 nM (0.75 ppb) and high sensitivity of 4.76 $\mu A \mu M^{-1}$, while the World Health Organization's guideline value of arsenic for drinking water is 10 ppb. It is worth to note that the electrode presents no interference from copper ion, which is the most serious interfering species in arsenic detection.

Key Words: Platinum-iron nanoparticles, Electrodeposition, Arsenic, Multiwalled carbon nanotube, Anodic stripping voltammetry

Introduction

The arsenic contamination in drinking water is unsafe and has been reported in some countries around the world.[1] Arsenic (As) is a highly toxic element and can cause various human diseases such as skin lesions, bladder and lung cancer, heart disease, keratosis, and stillbirth.[2-4] Two major forms of arsenic in water are arsenite (As(III)) and arsenate (As(V)). As(III) is 50 times more toxic than As(V) owing to As(III) reactions with enzymes in the human respiratory system.[2] The maximum permissible contaminant level of arsenic set by the World Health Organization (WHO) is 10 ppb (133 nM) in drinking water.[5]

Manny studies and techniques for the detection of arsenic have been published and developed. Some techniques such as inductively coupled plasma mass spectrometry,[6] hydride generation atomic fluorescence spectrometry,[7] and atomic absorption spectroscopy[8] showed good sensitivity and low limit of detection. However, disadvantages of using these techniques are expensiveness, difficulty to handle, and high operation costs, etc. Recently, many experiments are being performed using the electrochemical techniques and sensors to make up the disadvantages of arsenic detection at low concentrations. Several types of Hg electrode using stripping analysis[9] have been used for the detection of arsenic during the past two decades. The usage of mercury electrode brought about the difficulties in the treatment of the toxic metal. However, the development of sensors using metal nanoparticles is very promising and becoming an attractive study field in the electrochemical detection area. Nanometer-size materials have been used successfully for a wide range of electrochemical detection owing to their advantages such as fast mass transfer, sensitivity increase, catalytic effect, and large surface area.[10] While there are many ways in the preparation of metal nanoparticle, electrochemical deposition and chemical reduction technique have been widely used. Especially, the electrochemical deposition is fast and easy way to make a metal nanoparticle deposited electrode.[11]

In order to improve analytical ability for arsenic detection, a lot of effort has been put into modification of electrode surfaces and materials by using metal nanoparticles and carbon electrodes, including carbon nanotubes. Examples are Au-nanoparticle modified glassy carbon electrode (GCE),[12-14] Au modified boron doped diamond (BDD) electrode,[15,16] Au nanoparticle modified carbon nanotubes or carbon microspheres[17-19] and Au nanoelectrode ensembles.[20] Among other methods are silver electrode,[21] Platinum (Pt) nanoparticle modified GCE,[22] Pt nanotube,[23] Pt modified BDD electrode,[24] Iridium-implanted BDD electrode,[25] arsenite oxidase biosensor,[26] screen printed ring disk carbon electrode,[27] and cobalt oxide nanoparticle modified GCE.[28] Most studies using these modified electrodes adopted anodic stripping voltammetry (ASV) for more effective and sensitive detection of arsenic. Although these modified electrodes show the successful determination of As(III) with a low limit of detection (LOD) *via* anodic stripping voltammetry, their sensitivities remain relatively low level and they suffers from the problem of copper interference. Recently, some studies showed that using the deposited metal nanoparticles as alloy or metal oxide with another metal improved the electrochemical catalytic effects. For example, Lin et al. reported the cooperative effect of platinum nanoparicles and Fe(III) co-deposited on

†This paper is dedicated to Professor Hasuck Kim for his outstanding contribution to electrochemistry and analytical chemistry.

GCE in the electrocatalytic oxidation of nitrite and nitric oxide.[29-31] Therefore, the electrochemical co-deposition of Pt nanoparticles with transition metal oxide can be an alternative to increase sensitivity.

In this study, we have developed a novel platinum-iron(III) nanoparticles modified multiwall carbon nanotube-Nafion composite film on glassy carbon electrode (nanoPt-Fe(III)/MWCNT/GCE) for the electrochemical detection of As(III). In the experiment, Nafion, a perfluorinated sulfonate cation exchanger, was used as a polymeric binder of MWCNT onto the electrode surface. The Pt and iron(III) nanoparticles, incorporated within the MWCNT-Nafion composite film, co-deposited from the solution improves the electrocatalytic ability toward the electrochemical oxidation of As(III). The prepared electrode shows high sensitivity and low LOD and can be successfully used for the detection of As(III) using ASV without interference by copper ion. The optimum experimental conditions such as deposition time and applied potential were examined and the effect of co-deposition of other transition metal was also discussed.

Experimental

Materials and reagents. Potassium hexachloroplatinate(IV) (K_2PtCl_6, 98%), Iron(III) chloride ($FeCl_3$, 97%), Sodium (meta) arsenite ($NaAsO_2$,), Copper(II) chloride dihydrate ($CuCl_2{\cdot}2H_2O$, 99.9%), Cobalt(II) chloride ($CoCl_2$, 97%), Nickel(II) chloride hexahydrate ($NiCl_2{\cdot}6H_2O$, 99.9%) and Nafion (5 wt %) were purchased from Sigma-Aldrich (USA) and used without further purification. All other chemicals were of analytical grade and Multi-walled carbon nanotubes (MWCNT, 95% purity, diameter 10 ~ 15 nm, and length 10 ~ 50 μm) were purchased from Iljin (Korea). All solutions were prepared with deionized water obtained from Ultrapure water purification system (LabTech, Korea) with a resistivity of not less than 18.2 MΩcm.

Apparatus. Cyclic voltametry (CV) and linear sweep voltametry (LSV) were performed using a computer-controlled CHI 842B potentiostat with a conventional three-electrode system. A glass carbon (GC) working electrode (3 mm diameter) purchased from bioanalytical system (BAS) was used for the preparation of the modified electrode. A platinum (Pt) counter electrode and a silver/silver chloride (Ag/AgCl, 3 M KCl) reference electrode were used for the three-electrode system. Images of the modified electrode surface were obtained using a field emission scanning electron microscopy (FE-SEM, Hitachi S-48000) and atomic force microscopy (AFM, XE-70).

Preparation of GCE modified with Pt nanoparticles and Fe (III) (Pt-Fe(III)/GCE). A GC electrode was polished with aqueous slurries of successively finer aluminar (particle size : 0.3 and 0.05 μm) on polishing pad. The GC electrode was rinsed, then sonicated in deionized water and isopropyl alcohol for each 5 minute. After dried, the electrochemical co-deposition of Pt-Fe(III) nanoparticles on GCE was conducted in the solution containing 0.6 mM K_2PtCl_6, 0.4 mM $FeCl_3$ and 0.1 M KCl by repetitive potential cycling between 0.7 and −0.8 V at a scan rate of 50 mVs^{-1} for 30 cycles.[31] The optimum molar ratio (Pt:Fe = 3:2) used in the mixture solution for the electrodeposition of nanoparticles was reported in the previous studies.[29-31] Using the same molar ratio for other metals' co-electrodeposition with Pt, we prepared Pt-Metal/GCE (where, Metal = Co, Cu, Ni, Pd) with the same deposition method as described above. The modified electrode was washed with deionized water and dried at room temperature in the air.

Preparation of nanoPt-Fe(III)/MWCNT/GCE. The purification of MWCNT for modified electrode was adapted from previously published studies.[33,34] The 5 mg MWCNTs were purified by ultra-sonicator in 5 mL 3 M HNO_3 for 24 h. The obtained homogenous black suspension was filtered by membrane filter (pore size 0.2 μm). After rinsed using deionized water, it was dried at 70 °C in a drying oven. The dried 5 mg MWCNTs were agitated by ultra-sonicator in 5 mL 0.5 wt % Nafion solution for 1 h. Then, 10 μL of the obtained homogenous black suspension (Nafion-MWCNT mixture, 1 mg/mL MWCNT) was dropped by casting on purified GCE. After dried at room temperature in the air, the modified electrode was electrodeposited from solution containing 0.9 mM K_2PtCl_6, 0.6 mM $FeCl_3$ and 0.1 M KCl using potential cycling between 0.7 and −0.8 V at a scan rate of 50 mVs^{-1} for 5 cycles.

Results and Discussion

Fig. 1 shows the typical cyclic voltammetry responses of a bare GCE (curve a), Pt-Fe(III)/GCE in absence (curve b) and presence (curve c) of 0.1 mM As(III) in 0.1 M H_2SO_4 solution. As a result of electrochemical co-deposition of Pt and Fe(III) nanoparticles on bare GCE, the curve b as a background response shows a characteristic feature due to hydrogen adsorption and desorption on Pt nanoparicles in the potential region of 0 to −0.20 V in 0.1 M H_2SO_4 solution. Two main oxidation peaks are observed on the curve c at 0.39 V and 0.91 V in the presence of 0.1 mM As(III). The first oxidation peak at 0.39 V is attributed to the oxidation of As(0) to As(III) and the second one at 0.91 V corresponds to the oxidation of As(III) to As(V). The huge reduction peak observed at 0.29 V is typically due to the reduction of Pt oxide layer formed on the surface of Pt nanoparticles during the anodic scan.[35] In this study we focused on the second oxidation peak because the second peak current is more sensitive than the first one in the electrochemical detection

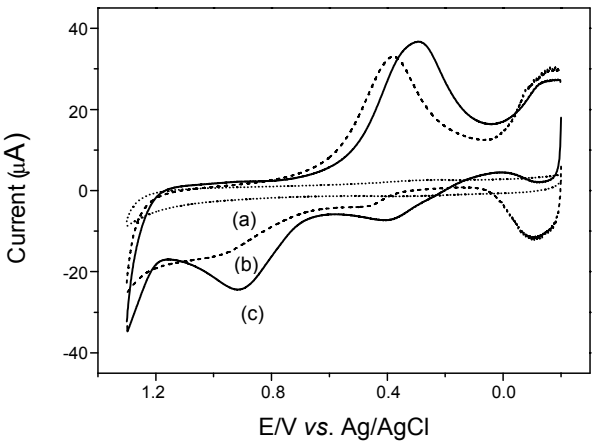

Figure 1. CV of the Bare GCE (a), Pt-Fe(III)/GCE (b, c) in absence (a, b) and presence(c) of 0.1 mM As(III) in 0.1 M H_2SO_4 solution at scan rate of 100 mVs^{-1}.

of arsenite. A straight line was also observed in the plot of the 2nd oxidation peak current of As(III) to As (*vs*. root of scan rate ($v^{1/2}$), indicating that the oxidation reaction is a diffusion process.

In order to look for the suitable electrode type for the arsenite detection, we compared the oxidation peaks of As(III) to As(V) observed from the modified electrodes in 0.1 M H_2SO_4 solution containing 0.1 mM As(III), shown in Fig. 2. There was no oxidation peak using the bare GCE (curve a), which means that bare GCE is not a good candidate. The oxidation peak currents measured at around 0.82 V on bare Pt electrode (curve b) and Pt nanoparticles electrodes (Pt/GCE) in curve c were 5.54 and 6.36 μA, respectively. Though their reduction peaks are different in shape and peak potential mainly due to the electrode microstructural difference, using metal nanoparticles' characteristics is an attractive approach to fabricate sensor electrode as reported[22] previously. However, the peak current on Pt-Fe (III)/GCE (curve d) after background correction was 8.60 μA, which is the largest among the modified electrodes. This fact demonstrates that the electrochemical co-deposition of Pt and Fe(III) on bare GCE can be a good approach for the detection of arsenic oxidation. Lin *et al*[30,31] reported that electrodeposition of Pt and Fe(III) nanoparticles exhibited excellent electrocatalytic activity for the oxidation of nitric oxide. In this study, the current enhancement result might be attributed to the cooperative effect of the composite Pt and Fe(III) mixed nanoparticles on bare GCE.

For the detection of arsenic oxidation, a good way to demonstrate the co-electrodeposition effect of Fe(III) in the mixed nanoparticles is to compare with voltametric results from co-deposition using other transition metal ion instead of Fe(III).

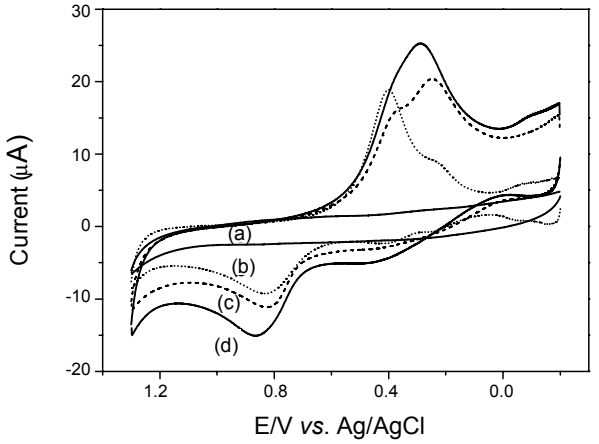

Figure 2. CV of the Bare GCE (a), bare Pt electrode (b), Pt/GCE (c) and Pt-Fe(III)/GCE (d) in 0.1 M H_2SO_4 solution containing 0.1 mM As(III) at scan rate of 100 mVs^{-1}.

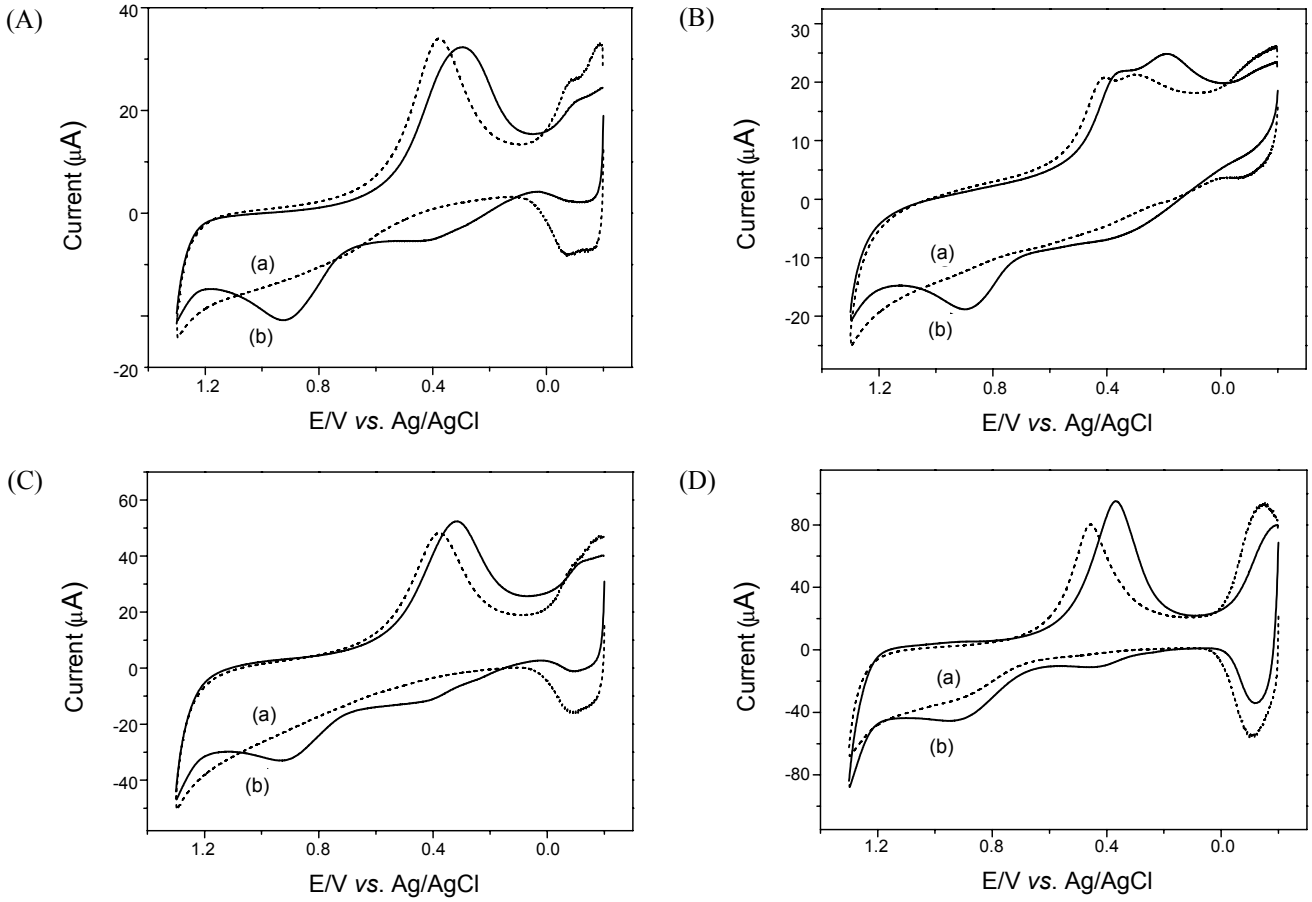

Figure 3. CVs of the Pt-Metal/GCE in absence (a) and presence (b) of 0.1 mM As(III) in 0.1 M H_2SO_4 solution at scan rate of 100 mVs^{-1}. metal: (A) Co, (B) Cu, (C) Ni, (D) Pd.

Table 1. The oxidation peak current of As(III) to As(V) on Pt-Metal (Fe, Co, Cu, Ni, Pd)/GCE in presence of 0.1 mM As(III) in 0.1 M H_2SO_4 solution

Electrode	Peak current (μA)
Pt-Fe(III)/GCE	13.21 ± 0.04
Pt-Co/GCE	10.49 ± 0.03
Pt-Cu/GCE	6.35 ± 0.70
Pt-Ni/GCE	9.50 ± 0.75
Pt-Pd/GCE	12.51 ± 0.46

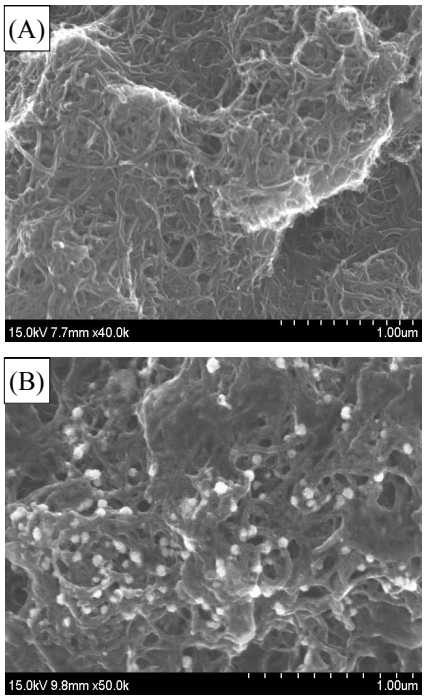

Figure 4. FE-SEM images for the surface of MWCNT dispersed in Nafion composite on bare GCE before (A) and after (B) Pt-Fe(III) co-electodeposition.

To evaluate the co-deposition effect, we prepared four different types of Pt-Metal/GCEs in which Pt was electrodeposited with cobalt, copper, nickel, and palladium metal ions, respectively. Electrodeposition process was accomplished using fresh solution mixtures, which contains the same molar concentration of four different metal ions compared to that of Pt (molar ratio of Pt:Metal = 3:2). Fig. 3 shows typical cyclic voltammetry responses of Pt-Metal (Co, Cu, Ni, Pd)/GCE in the absence (curve a) and presence (curve b) of 0.1 mM As(III) in 0.1 M H_2SO_4 solution.

All of the electrodes modified with co-electrodeposition show almost the same voltammetric features as observed at Pt-Fe(III)/GCE (shown in Fig. 2d). As shown in Fig. 3, the respective oxidation of As(III) takes place at quite similar peak potential of *ca*. 0.91 V irrespective of co-deposited metal. However, the oxidation peak currents measured at the modified GCEs are slightly different each other. The differences in the oxidation current might be due to the electrocatalytic cooperative activity of co-deposited metals, coming from several factors such as size, shape, and microstructure of metal nanoparticles.

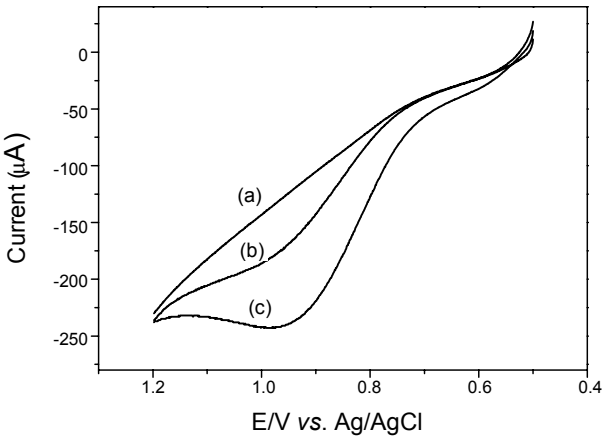

Figure 5. LSV of the nanoPt-Fe(III)/MWCNT/GCE in 0.1 M H_2SO_4 solution containing concentration of As(III): (a) 0 mM, (b) 0.1 mM, (c) 0.3 mM.

After the background correction, the oxidation peak current of As(III) at the modified electrodes including Pt-Fe(III)/GCE were averaged from three times measurements and summerized in Table 1. On the whole Pt-Fe(III)/GCE and Pt-Pd/GCE seem to be more sensitive than other Pt-Metal/GCEs for the detection of As(III) oxidation.

Recently, Tsai and Hong[32] reported the electrochemical deposition of Pt nanoparticles in MWCNT-Nafion composite for methanol electrooxidation. This approach looks promising to develop a novel sensor for a wide range of sensing applications. In order to improve electrocatalytic ability toward the electrochemical oxidation of As(III), Pt and Fe(III) nanoparticles were simultaneously electrodeposited by repetitive potential cycling into the MWCNT-Nafion nanocomposite film on bare GCE. Fig. 4 shows the FE-SEM images of MWCNT-Nafion nanocomposite before and after electrodeposition of Pt and Fe(III) nanoparticles on GCE. The Pt nanoparticles were deposited to the surface of MWCNT, which is a pathway for electrons to carry out electrodeposition reaction and provides good electric contact with bare GCE through the Nafion composite film.

As shown in the FE-SEM images, the nanoparticles with the diameter of about 70 nm are distributed on the surface of MWCNT well-dispersed in Nafion membrane. The nanoparticles in the FE-SEM image are not an alloy of Pt and Fe(III) but Pt nanoparticles. According to the previous reports,[30,31] the chemical identity of Fe(III) in the electrodeposition is known as the amorphous iron oxides and hydroxide species of Fe(III). In addition, the growth of Pt nanoparticles was limited by the Fe-O-Fe netting linkage.[31]

To test whether it is possible to use nanoPt-Fe(III)/MWCNT/GCE for the electrochemical detection of As(III), we first hired linear sweep voltammetry. Fig. 5 shows linear sweep voltammograms of nanoPt-Fe(III)/MWCNT/GCE in 0.1 M H_2SO_4 solution containing 0.1, 0.3 mM As(III) at scan rate of 100 mVs^{-1}. The oxidation peak currents measured at ca. 0.95 V were 34.71 and 89.84 μA in 0.1 and 0.3 mM As(III), respectively. These values are expected to be high at relatively low concentration of arsenite.

In order to find out optimum conditions for more sensitive

anodic stripping voltammetry experiments, ASV was performed using nanoPt-Fe(III)/MWCNT/GCE. The measurement of ASV starts from the deposition potential after holding the potential at the deposition potential. Fig. 6A shows the effect of deposition potential at constant deposition time of 120 s on the anodic stripping current of As(III). The higher oxidation current was measured as the deposition potential became more negative. However, at more negative potentials than −0.3 V, the oxidation peak current was decreased due to the interference of hydrogen evolution on the nanoPt-Fe(III)/MWCNT/GCE surface. Therefore, −0.3 V was determined to be an optimum and used in further experiments. Fig. 6B illustrates the effect of deposition time at constant deposition potential of −0.3 V. The oxidation peak current of As(III) was increased with increasing deposition time, but the oxidation peak current reached a constant value after 180 s. Furthermore, the nanoPt-Fe(III)/MWCNT/GCE seemed to be damaged with longer deposition time. Therefore, 180 s was determined to be an optimum deposition time for the detection of As(III).

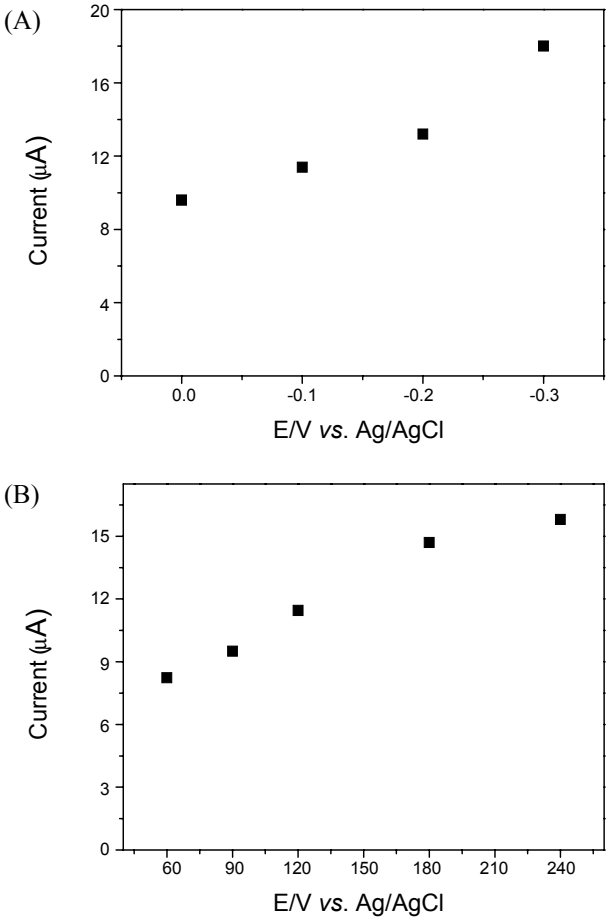

Figure 6. Optimization experiments of ASV using the nanoPt-Fe(III)/MWCNT/GCE in 0.1 M H_2SO_4 solution containing 5 μM As(III) at scan rate of 100 mVs^{-1}. (A) Effect of predeposition potential (constant time: 120 s), (B) Effect of predeposition time (constant potential: −0.3 V).

Fig. 7 shows that ASV responses of the nanoPt-Fe(III)/MWCNT/GCE at various concentration of As(III) in 0.1 M

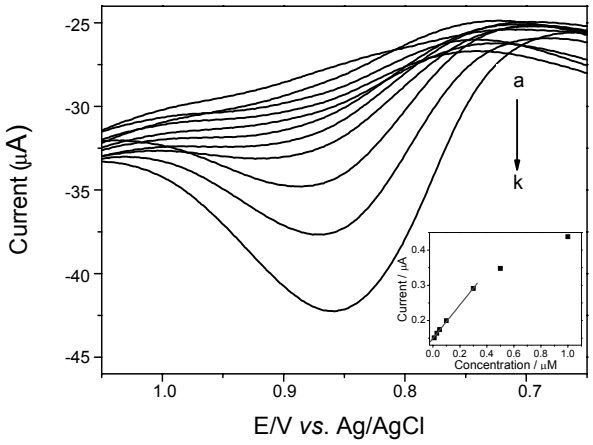

Figure 7. ASV of the nanoPt-Fe(III)/MWCNT/GCE in 0.1 M H_2SO_4 solution containing various concentration of (a) 0, (b) 0.01, (c) 0.03, (d) 0.05, (e) 0.1, (f) 0.3, (g) 0.5, (h) 1, (i) 3, (j) 5, (k) 10 μM As(III) at scan rate of 100 mVs^{-1}(predeposition condition: −0.3 V, 180 s). Insert: the calibration curve of current *vs*. concentration of As(III).

Table 2. Detection studies of Arsenic using diverse electrode and technique. (SPRDE: screen printed ring disk carbon electrode, FIA: flow injection analysis, ASV: anodic stripping voltammetry, ABS: acetate buffer solution, GC-CNT/Au-np-GC: glassy carbon electrode with gold nanoparticle modified glassy carbon sphere, LSV: linear sweep voltammetry, CV: cyclic voltammetry, BDD: boron doped diamond electrode, PBS: phosphate buffer solution, MWCNT: multiwalled carbon nanotube, GCE: glassy carbon electrodes, Aro: arsenite oxidase, PtNTAE: platinum nanotube array electrode)

Electrode	Technique	Electrolyte	Linearity of response up to (μM)	Sensitivity (μA/μM)	LOD (ppb)	Reference
SPRDE	FIA (ASV)	0.1 M ABS (pH 4)	10	0.014	5.24	26
GC-CNT/Au-np-GC	ASV-LSV	1 M H_2SO_4	-	6	2.5	18
Au nanoparticles coated BDD	ASV-CV	0.1 M PBS (pH 7)	-	-	1	15
Au coated BDD	ASV-LSV	0.1 M PBS (pH 5)	0.4	-	5	14
Ir implanted BDD	FIA	0.1 M PBS (pH 4)	100	0.0065	1.5	24
nano-Au/GCE	ASV-LSV	3 M HCl	-	2.5	1.8	12
MWCNT/Aro/GCE	CV, Amperometry	0.1 M PBS (pH 7)	6.67	0.107	1	25
PtNTAE	LSV	0.1 M H_2SO_4	200	0.8	0.1	22
nanoPt modified GCE	CV, ASV-LSV	0.1 M H_2SO_4	50	0.22	2.1	21
nanoCo modified GCE	CV, Amperometry	0.1 M PBS (pH 7)	4	0.111	0.83	27
nanoPt-Fe(III)/MWCNT/GCE	**ASV**	**0.1 M H_2SO_4**	**0.3**	**4.76**	**0.75**	**This study**

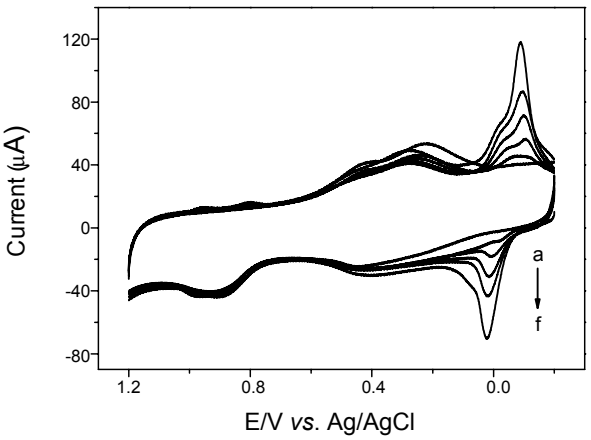

Figuer 8. CV of Cu(II) addition (a) 0, (b) 0.02, (c) 0.04, (d) 0.06, (e) 0.08, (f) 0.1 mM in 0.1 M H_2SO_4 solution containing 0.1 mM As(III) on the nanoPt-Fe(III)/MWCNT/GCE at scan rate of 100 mVs^{-1}.

H_2SO_4 solution at scan rate of 100 mVs^{-1} under optimal deposition conditions. The oxidation peak current of As(III) was increased with increasing concentration of As(III). In the anodic stripping scan, two main oxidation peaks are typically observed at 0.39 V and 0.91 V after the deposition of As(0) at −0.3 V. The first oxidation peak at 0.39 V is attributed to the oxidation of As(0) to As(III) and the second one at 0.91 V corresponds to the oxidation of As(III) to As(V). We used the second oxidation peak current to detect arsenic due to its higher current density. Inset is the calibration curve of the oxidation peak current *vs*. concentration of As(III). The sensitivity was estimated to be 4.76 $\mu A \mu M^{-1}$ and the limit of detection(LOD, S/N = 3) was 10 nM (0.75 ppb). The Linearity of the response was up to 0.3 μM with a correlation coefficient of 0.9992.

And the results of arsenic detection by ASV using the nano-Pt-Fe(III)/MWCNT/GCE were compared with other values of arsenic detection reported in recent studies (Table 2). One of the most attractive features of the arsenic detection by ASV using the nanoPt-Fe(III)/MWCNT/GCE is high sensitivity. Although linear range in this study is smaller than other studies, the advantages of high sensitivity and low LOD seem to outweigh the disadvantage. Using nanoPt-Fe(III)/MWCNT/GCE, As(III) can be detected at the level of 10 nM, 0.75 ppb, which is much lower than the level set by WHO (133 nM, 10 ppb), *via* ASV.

Among the possible interference metals, Cu(II) is the most common and ubiquitous in water systems and is found in relatively high levels with detection of arsenic(III).[36] Therefore, we carried out cyclic voltammetry experiments to evaluate the interference effect of Cu(II) species. Fig. 8 shows cyclic voltammetry responses upon five times Cu(II) addition (20 μM each) at the nanoPt-Fe(III)/MWCNT/GCE in 0.1 M H_2SO_4 containing 0.1 mM As(III). The peak currents of a pair of redox peaks at *ca*. 0.02 and −0.10 V were increased with the addition of Cu(II). However, the oxidation peak height of As(III) to As(V) around 0.9 V was not changed even though Cu(II) was added to the solution. This fact demonstrates that Cu(II) does not have any interference to the oxidation of As(III) using the nanoPt-Fe(III)/MWCNT/GCE.

Conclusion

This study shows that the platinum and Fe(III) nanopaticles can be easily electrodeposited in the MWCNT-Nafion nanocomposite film on bare GCE and the electrode system can be used for the electrochemical detection of arsenic(III) *via* anodic stripping-linear sweep voltammetry. The oxidation of As(III) to As(V) based on the electrocatalytic cooperative effect of Pt-Fe(III) nanoparticles is fast and sensitive for the quantitative determination of arsenic(III). A high sensitivity as well as limit of detection (0.75 ppb) which is much lower than the recommended level (10 ppb) set by WHO in drinkable water were achieved. It was found that the nanoPt-Fe(III)/MWCNT/GCE can be used without interference of copper in the determination of As(III).

Acknowledgments. This work was supported by the Korea Research Foundation funded by the Korean Government (MOEHRD), Basic Research Promotion Fund (KRF-2008-314-C00235).

Reference

1. World Health Organization, United Nations Synthesis Report on Arsenic in Drinking Water, http://www.who.int/water_sanitation_health/dwq/arsenic3/en/
2. Mandal, B. K.; Suzuki, K. T. *Talanta* **2002**, *58*, 201.
3. Smith, A. H.; Lingas, E. O.; Rahman, M. *Bulletin of the World Health Organization*. **2000**, *9*, 1093.
4. Mukherjee, A.; Sengupta, M. K.; Hossain, M. A.; Ahamed, S.; Das, B.; Nayak, B.; Lodh, D.; Rahman, M. M.; Chakraborti, D. *J. Health. Popul. Nutr.* **2006**, *24*, 142.
5. World Health Organization, Arsenic in drinking water, http://www.who.int/mediacentre/factsheets/fs210/en/index.html, RevisedMay-2001
6. Nam, S. H.; Kim, J. J.; Han S. S. *Bull. Korean Chem. Soc.* **2003**, *24*, 1805.
7. Lopez, A. C.; Castro, M. D. L. *Anal. Chem*. **2003**, *75*, 2011.
8. Hung, D. Q.; Nekrassova, O.; Compton, R. G. *Talanta* **2004**, *64*, 269.
9. Wang, S. *Stripping Analysis: Principles, Instrumentation, and Applications*; VCH Publishers: 1985.
10. Santos, D. H.; Garcia, M. B. G.; Garcia, A. C. *Electroanalysis* **2002**, *14*, 1225.
11. Mays, D. E.; Hussam, A. *Anal. Chim. Acta* **2009**, *646*, 6.
12. Majid, E.; Hrapovic, S.; Liu, Y.; Male, K. B.; Luong, J. H. T. *Anal. Chem*. **2006**, *78*, 762.
13. Hossain, M. M.; Islam, M. M.; Ferdousi, S.; Okajima, T.; Ohsaka, T. *Electroanalysis* **2008**, *20*, 2435.
14. Dai, X.; Compton, R. G. *Electroanalysis* **2005**, *17*, 14.
15. Yamada, D.; Ivandini, T. A.; Komatsu, M.; Fujishima, A.; Einaga, Y. *J. Electroanal. Chem*. **2008**, *615*, 145.
16. Rassaei, L.; Sillanpaa, M.; French, R. W.; Compton, R. G.; Marken, F. *Electroanalysis* **2008**, *20*, 1286.
17. Xiao, L.; Wildgoose, G. G.; Compton, R. G. *Anal. Chim. Acta* **2008**, *620*, 44.
18. Baron, R.; Sljukic, B.; Salter, C.; Crossley, A.; Compton, R. G. *Russian Journal* of *Physical Chemistry A* **2007**, *81*, 9.
19. Dai, X.; Wildgoose, G. G.; Salter, C.; Crossley, A.; Compton, R. G. *Anal. Chem*. **2006**, *78*, 6102.
20. Jena, B. K.; Raj, C. R. *Anal. Chem*. **2008**, *80*, 4836.
21. Simm, A. O.; Banks, C. E.; Compton, R. G. *Electroanalysis* **2005**, *17*, 1727.
22. Dai, X.; Compton, R. G. *Analyst* **2006**, *131*, 516.
23. Xu, H.; Zeng, L.; Xing, S. J.; Shi, G. Y.; Chen, J.; Xian, Y. Z.; Jin,

L. *Electrochem. Commun.* **2008**, *10*, 1893.
24. Hrapovic, S.; Liu, Y.; Luong, J. H. T. *Anal. Chem.* **2007**, *79*, 500.
25. Ivandini, T. A.; Sato, R.; Makide, Y.; Fujishima, A.; Einaga, Y. *Anal. Chem.* **2006**, *78*, 6291.
26. Male, K. B.; Hrapovic, S.; Santini, J. M.; Luong, J. H. T. *Anal. Chem.* **2007**, *79*, 7831.
27. Sue, J. W.; Ku, H. H.; Chung, H. H.; Zen, J. M. *Electrochem. Commun.* **2008**, *10*, 987.
28. Salimi, A.; Mamkhezri, H.; Hallaj, R.; Soltanian, S. *Sensors and Actuators B* **2008**, *129*, 246.
29. Wang, S.; Lu, L.; Lin, X. *Electroanalysis* **2004**, *16*, 20.
30. Wang, S.; Yin, Y.; Lin, X. *Electrochem. Commun.* **2004**, *6*, 259.
31. Wang, S.; Lin, X. *Electrochimica Acta* **2005**, *50*, 2887.
32. Tsai, Y. C.; Hong, Y. H. *J. Solid State Electrochem.* **2008**, *12*, 1293.
33. Zhang, M.; Su, L.; Mao, L.; *Carbon* **2006**, *44*, 276.
34. Wang, J.; Yin, G.; Shao, Y.; Wang, Z.; Gao, Y. *J. Electrochem. Soc.* **2007**, *154*, 687.
35. Brusciotti, F.; Duby, P. *Electrochimica Acta* **2007**, *52*, 6644.
36. Anawar, H. M.; Akai, J.; Mostofa, K. M. G.; Safiullah, S.; Tareq, S. M. *Environ, Int.* **2002**, *27*, 597.